Journal of Non-Crystalline Solids 292 (2001) 115–126

Highly bioactive P_2O_5–Na_2O–CaO–SiO_2 glass-ceramics

Oscar Peitl [a,*], Edgar Dutra Zanotto [a], Larry L. Hench [b]

[a] *Vitreous Materials Laboratory (LaMaV), Department of Materials Engineering (DEMa), Federal University of São Carlos (UFSCar), CP. 676, CEP 13565-905, São Carlos, SP, Brazil*
[b] *Department of Materials, Imperial College, London SW7 2BP, UK*

Received 15 December 1999; received in revised form 2 July 2001

Abstract

Glasses having a chemical composition between $1Na_2O$–2CaO–$3SiO_2$ (1N2C3S) and $1.5Na_2O$–1.5CaO–$3SiO_2$, containing 0, 2, 4 and 6 wt% P_2O_5, were crystallized to several volume percent through thermal treatments in the range 550–700 °C. These glasses and glass-ceramics were exposed to a simulated body fluid solution (SBF-K9 which is close to human plasma) for several time periods. Fourier transform infrared spectroscopy (FTIR) was used to determine the rate of hydroxy carbonate apatite (HCA) formation. Crystallization decreased the kinetics but did not inhibit the development of a HCA layer, even in fully crystallized ceramics. The onset time for crystallization of HCA varied from 8 h for a glass containing 6% P_2O_5 to 35 h for a fully crystallized $1.07Na_2O$–2CaO–$3SiO_2$ ceramic. The HCA layer formation of these compositions in 'in vitro' tests is much faster than in commercial bioactive materials such as synthetic hydroxyapatite ceramic, A/W glass-ceramic, Ceravital and Bioverit, for which the onset time usually takes at least seven days. FTIR and inductive coupled plasma studies confirmed the formation of an apatite layer which indicates bioactivity in the 1N2C3S crystal phase. X-ray diffraction experiments show that the phosphorus ions are kept in solid solution in the crystal phase. An apatite-like compound only appeared when the specimens were submitted to very long additional thermal treatments. The bioactivity of commercial materials is based on the apatite crystal phase, while the high level of bioactivity of this new generation of glass-ceramics is attained due to the combination of two mechanisms acting simultaneously; a non-phosphate bioactive crystal phase (1N2C3S) and the phosphorus ions in solid solution which are easily released from the structure, promoting a faster HCA layer formation similar to 45S5 Bioglass®.

1. Introduction

Previous studies have shown that crystallization decreases the level of bioactivity [1] and can even turn a bioactive glass into an inert material [2]. A bioactive material is considered as the one that elicits a specific biological response at the interface that results in the formation of a bond between the tissues and the material. However, it should be stressed that bioactivity is not only a material property but also depends on the solution used for in vitro tests. Many efforts have been made by researchers to understand the effect of solution type and material composition on hydroxyl carbonate apatite (HCA) layer formation [3–10]. For example, Kokubo et al. [11] have shown that a tris-buffer solution did not produce HCA on an A/W glass-ceramic. However, exposure to a simulated body fluid produced a HCA layer. Kokubo et al.

* Corresponding author. Tel.: +55-16 260 8250; fax: +55-16 261 5404.
E-mail address: opeitl@power.ufscar.br (O. Peitl).

0022-3093/01/$ - see front matter
PII: S0022-3093(01)00822-5

[11] developed a series of acellular aqueous solutions which are able to reproduce in vivo surface–structure changes in bioactive materials. The SBF-K9 solution is the closest to human plasma, as shown in Table 1.

Most articles deal with a single glass composition or one specific glass-ceramic; few papers study the effect of crystallization on the rate of HCA layer formation. For instance, Peitl et al. [1] and Li et al. [2] have found opposite results. Li et al. [2] showed that a bioactive glass can be transformed into an inert glass-ceramic. He found a HCA layer formation using in vitro tests, only if the glass-ceramic contained a high proportion (over 90%) of a residual glassy phase. However, Peitl et al. [1] have shown that crystallization of Bioglass® 45S5 did not inhibit HCA formation in an in vitro test with SBF-K9, even with a fully crystallized glass-ceramic. The onset time for HCA layer formation did decrease with increased crystallinity in Peitl et al. [1] study.

The objective of this paper is to establish the structural basis for the effect of crystallinity on the rates of HCA formation in vitro.

2. Reaction sequence

Studies of HCA layer formation on the surface of bioactive materials have shown that reactions occur on the material side in five stages. These stages are fastest for the highest level of bioactivity [12]. Surface reaction stages I–V on a bioactive glass in aqueous solution [3–5] are summarized below:

Stage (I). Rapid exchange of Na^+ or K^+ with H^+ or H_3O^+ from solution,

$$\text{Si–O–Na}^+ + \text{H}^+ + \text{OH}^- \Rightarrow \text{Si–OH} + \text{Na}^+_{(\text{solution})} + \text{OH}^-.$$

Stage (II). Loss of soluble silica in the form of $Si(OH)_4$ to the solution resulting from breakage of Si–O–Si bonds and formation of Si–OH (silanols) at the glass solution interface:

$$2(\text{Si–O–Si}) + 2(\text{OH}) \Rightarrow \text{Si–OH} + \text{OH–Si}.$$

Stage (III). Condensation and repolymerization of an SiO_2 rich layer on the surface that is depleted in alkalis and alkaline earth cations.

$$2(\text{Si–OH}) + 2(\text{OH–Si}) \Rightarrow \text{–Si–O–Si–O–Si–O–Si–O–}.$$

Stage (IV). Migration of Ca^{2+} and PO_4^{3-} groups to the surface through the SiO_2-rich layer forming a $CaO–P_2O_5$-rich film on top of the SiO_2-rich layer, followed by growth of an amorphous $CaO–P_2O_5$-rich film by incorporation of soluble calcium and phosphate from solution.

Stage (V). Crystallization of the amorphous $CaO–P_2O_5$ film by incorporation of OH, CO_3^{2-}, or F anions from solution to form a mixed HCA layer or hydroxyl fluorapatite (HCFA) layer.

The characteristic double layer formation (stages I–V) on the surface of a bioactive glass is schematically shown in Fig. 1.

A common characteristic of bioactive glasses and glass-ceramics is the formation of a biological layer that bonds to the bone [12]. The kinetic reaction sequence depicted, stages I–V, can be followed with Fourier transform infrared spectroscopy (FTIR) [13,14].

There are large differences in the rate of bone bonding to bioactive implants (stages I–V) that depend on chemical composition, amount of glass phase and solubility, etc. [12]. According to Hench [15], bioactive materials are classified into two classes: Class A is osteoproductive and Class B is osteoconductive [15]. Class A elicits bone and soft tissue bonding and class B only shows bone

Table 1
Ion concentration (mM) in SBF-K9 and in human blood plasma [11]

Ion	Na^+	K^+	Mg^{2+}	Ca^{2+}	Cl^-	HCO_3^-	HPO_4^{2-}	SO_4^{2-}
SBF-K9	142.0	5.0	1.5	2.5	147.8	4.2	1.0	0.5
Human plasma	142.0	5.0	1.5	2.5	103.0	27.0	1.0	0.5

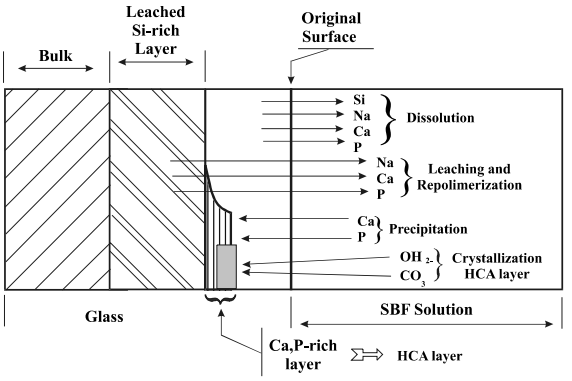

Fig. 1. Schematic illustration of the surface stages (I–V) reactions on bioactive glass, forming double SiO_2-rich and Ca, P-rich layers.

bonding [15]. Class A releases Si in the form of silicic acid due to ion exchange and network dissolution, and rapidly provides a silica-gel layer that accelerates the precipitation of amorphous calcium phosphate that, in turn, rapidly crystallizes HCA (1–10 h on SBF-K9). Class B has low or zero rate of Si ion exchange or network dissolution and only forms HCA from 100 h [15] in vitro tests.

3. Experimental

High purity silica and reagent-grade calcium carbonate, sodium carbonate and sodium phosphate were used to obtain glass compositions SS, 1.07N2C3S, SSP2, SSP4 and SSP6. Nominal compositions are given in Table 2.

Raw materials were weighed and mixed for four hours in a polyethylene bottle. Premixed batches were melted in a covered Pt crucible at the temperature range 1320–1370 °C for 4 h. Samples were cast into a graphite mold to form 8 mm × 30 mm cylinders. After annealing at 460 °C for 8 h the cylinders were cut into disks. The disks were heat-treated in two steps for nucleation and subsequent crystal growth. The crystal phases grown in the fully crystallized glass-ceramics were determined by X-ray diffraction (XRD). Combinations of time and temperature were used for nucleation and growth treatments to produce different volume fractions crystallized. Quantitative microstructure evaluations were obtained with an optical microscope using a point-counting stereology method. Table 3 shows the thermal treatments and the resulting volume percent crystallized for each composition.

Table 2
Glass compositions studied (wt%) [16]

Component	SiO_2	Na_2O	CaO	P_2O_5
1.07N2C3S	50.3	18.5	31.3	
SS	50.5	24.8	24.8	
SSP2	49.5	24.2	24.2	2.0
SSP4	48.5	23.8	23.8	4.0
SSP6	47.5	23.2	23.2	6.0
Bioglass®-45S5 [4]	45	24.5	24.5	6.0

Table 3
Thermal treatment ranges used to produce different crystal volumes

Composition	Nucleation		Growth		Volume (%)
	Temp. (°C)	Time (min)	Temp. (°C)	Time (min)	crystallized
1.07N2C3S	600	960	690	60	100
SS	520–560	3–180	620–640	6–22	10–100
SSP4	540–590	30–6000	650–700	5–80	5–100
SSP6	540–590	60–9000	650–700	10–70	10–100

All glass and glass-ceramic disks used for in vitro tests were prepared by wet grinding with 400-grit silicon carbide paper followed by dry grinding with 600-grit paper. Polished samples were cleaned in an acetone bath and air-dried. An SBF-K9 solution was prepared by mixing sodium chloride, sodium bicarbonate, potassium chloride, calcium chloride, dibasic potassium phosphate and magnesium chloride in deionized water, according to the method proposed by Kokubo et al. [11]. In vitro test samples were performed under static conditions soaking in sealed polyethylene bottles with SBF-K9 solution at 37 °C. The surface area to volume ratio (SA/V) was 0.1 cm^{-1} [17] and the treatment times varied from 1 to 96 h.

The glass and glass-ceramic disks were analyzed by FTIR spectroscopy before and after exposure to the SBF-K9 solution. The equipment used was a spectrometer with a diffuse reflectance stage. Spectra were obtained between 1400 and 400 cm^{-1} at 2 cm^{-1} resolution using a triglycerin sulfate (TGS) detector. Si, Ca and P concentrations were analyzed in the same reacted solutions by induced coupled plasma spectroscopy (ICP). Detection limits for Si and $P > 0.1$ ppm and $Ca > 0.01$ ppm.

4. Results

XRD spectra of 1.07N2C3S, SS, SSP4 and SSP6 glass-ceramics are shown in Fig. 2. The crystal phase in all glass-ceramics is $Na_2Ca_2Si_3O_9$ (1N2C2S). Both angular location and intensity of the peaks match quite well the standard PDF # 22.1455. No difference is observed between the quasi-stoichiometric composition, 1.07N2C3S, and SSP6, which is closest to Bioglass® 45S5. The crystal phase observed in the phosphorous-free glass-ceramics agrees with the findings of Moir and Glasser [18]. They showed that the 1N2C3S crystal phase displays an extended solid solution range that includes both 1.07N2C3S and SS compositions. The presence of up to 6.0% phosphorous was not enough for the precipitation of another crystal phase in SSP4 and SSP6. However, Li et al. [2] have found an apatite-like phase, $Ca_{10}(PO_4)_6$, in a partially crystallized glass-ceramic having 48 SiO_2, 9.5 P_2O_5, 20 Na_2O and 22.5 CaO (wt%).

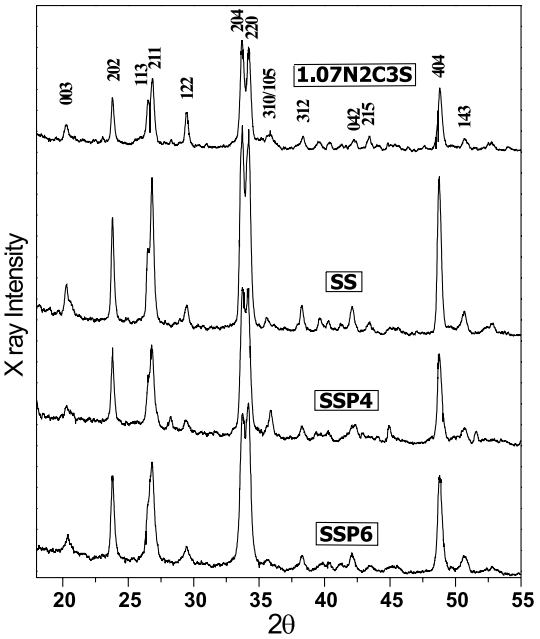

Fig. 2. XRD for fully crystallized SS, SSP4, SSP6 and 1.07N2C3S glass-ceramics.

The spectral peak assignments for the molecular vibrations observed in the FTIR analyses have been discussed previously [8,14]. The regions of special interest are listed in Table 4.

The FTIR spectra of SSP6 glass and fully crystallized 1.07N2C3S glass-ceramic, from unreacted to 96 h exposure in SBF, are shown in Figs. 3 and 4. The two most noticeable changes in the spectra when compared to the unreacted glass and 1.07N2C3S glass-ceramic are:

1. the original broad glass peaks at 1050, 910 and 490 cm^{-1} are decomposed into several narrow peaks and,
2. a new peak emerges at 575 cm^{-1}. These changes of vibrational modes may be attributed to the development of a crystal phase.

The vibrational modes changed as a function of reaction time in the SBF-K9 solution. Both materials developed a HCA layer on the surface (stage V). The appearance of HCA on the SSP6 glass was faster and took only 8-h exposure. The

Table 4
Infrared frequencies for functional groups in a bioactive glass [8,14]

Wavenumber (cm^{-1})	Vibrational mode	
1350–1080	P=O	Stretch
940–860	Si–O–Si	Stretch
890–800	C–O	Stretch
1175–710	Si–O–Si	Tetrahedral
610–600	P–O	Bend/crystal
560–550	P–O	Bend/glass
530–515	P–O	Bend/crystal
540–415	Si–O–Si	Bend

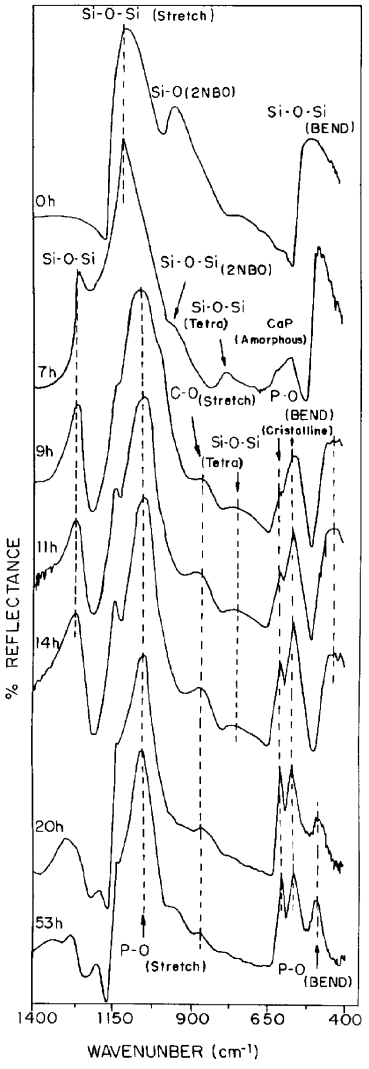

Fig. 3. FTIR spectra of glass SSP6 composition reacted from 0 to 53 h on SBF-K9 solution.

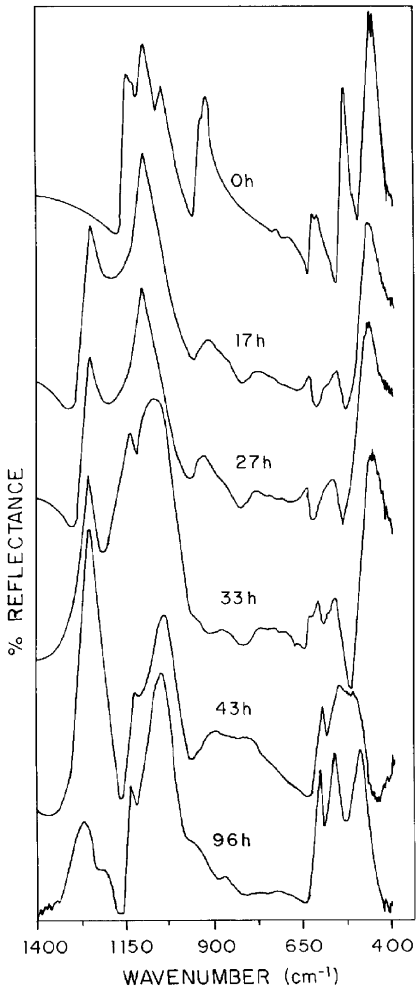

Fig. 4. FTIR spectra of fully crystallized 1.07N2C3S glass-ceramic reacted from 0 to 96 h on SBF-K9 solution.

glass-ceramic spectra, Fig. 4, show the evolution of surface reactions as a function of exposure time in SBF. The changes are similar to those of SSP6 glass; they are somewhat slower but lead to HCA formation. All IR peaks due to glass crystallization disappear after 33 h. The 33 h spectrum is comparable to the SSP6 glass spectrum after 11 h in SBF (Fig. 3).

The onset time of HCA crystallization was measured to establish the effect of volume percent crystallization and chemical composition on the bioactivity. Fig. 5 shows the HCA onset time for all compositions and crystallinities studied, which

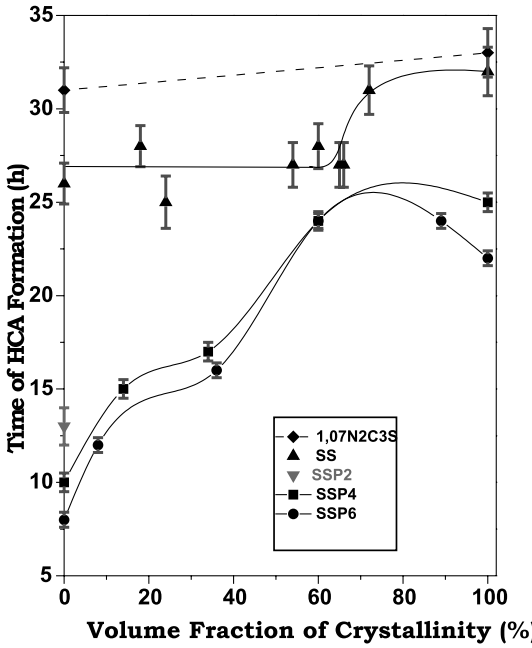

Fig. 5. Onset time HCA formation, stage V, with percent crystallization of glass-ceramics.

summarizes more than 250 in vitro bioactivity tests.

Fig. 5 shows that the presence of phosphorous in the glasses or glass-ceramics increases the rate of HCA formation (stages I–V). There is no significant difference between compositions with 4.0% and 6.0% P_2O_5, based upon student's T test analysis of the data. The SSP6 glass was the fastest to form a HCA layer (8 h) because its composition is very close to the 45S5 Bioglass® [5], the most bioactive commercial material produced so far, for which HCA formation starts after 6 h [8] in SBF-K9 solution. Crystallization of glasses SSP4 or SSP6 increases the onset time for HCA formation to 24 h, which is three times longer than for the original glass. However, crystallization of the phosphorous-free compositions, 1.07N2C3S and SS, had only a slight effect on the onset time for HCA layer formation (from 26 to 32 h). Thus, it is clear that glasses and glass-ceramic compositions *without phosphorous*, belonging to the 1N2C3S solid solution range, have almost the same bioactivity level.

The levels of Si, Ca and P, and the pH of a SBF-K9 solution after various times of immersion during in vitro tests were determined for 45S5 Bioglass®, 1.07N2C3S glass, glass-ceramic and partially crystallized ($\alpha = 34\%$) SSP4; results are shown in Figs. 6–9. Crystallization had only a small effect on the rate of ion release of the two systems (see for instance the 1.07N2C3S glass and glass-ceramic), even when there is a difference in the amount of P_2O_5 in the glass, from 6% to 4% (45S5 and SSP4; $\alpha = 34\%$). However, Fig. 6 shows that when materials with and without phosphorous are compared, the compositions with phosphorous are much more soluble and thus the concentration of Si in the SBF solution increases much more rapidly.

Calcium ions are also released faster from compositions with phosphorous (Fig. 8) especially in reaction stages I and II. Compositions with phosphorous reach a maximum in solubility of Ca; composition without phosphorous continuing to

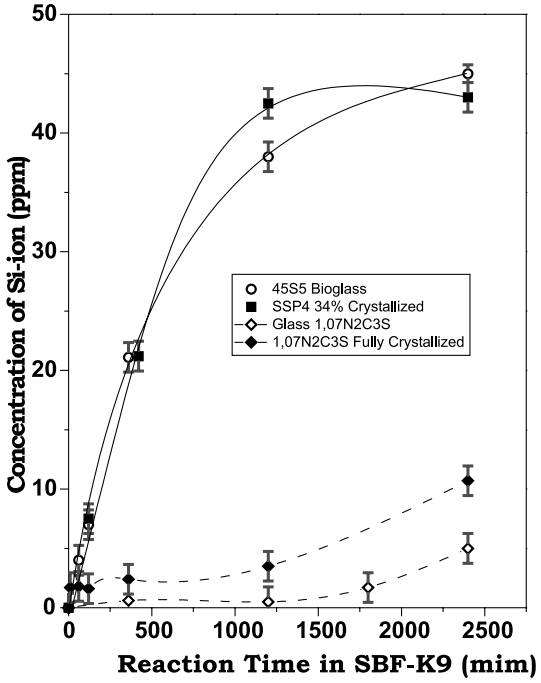

Fig. 6. Silicon ion concentration in reacted SBF-K9 solution for 45S5 Bioglass, SSP4 partially crystallized and 1.07N2C3S glass and glass-ceramic vs. reaction time.

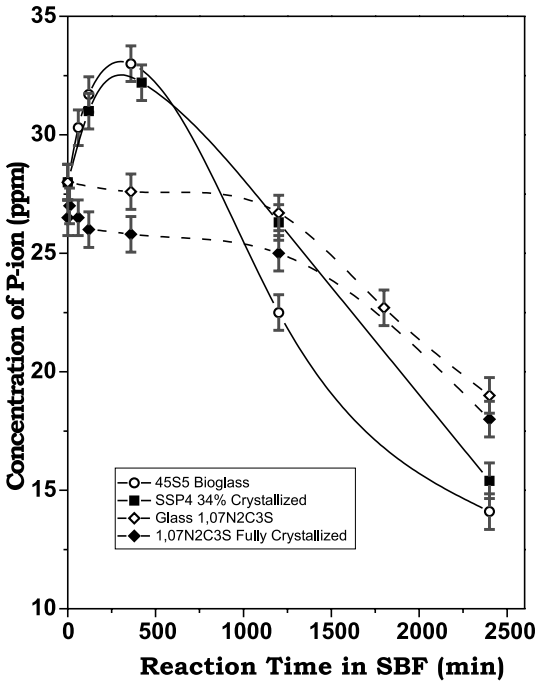

Fig. 7. Phosphorous ion concentration in reacted SBF-K9 solution for 45S5 Bioglass, SSP4 partially crystallized and 1.07N2C3S glass and glass-ceramic vs. reaction time.

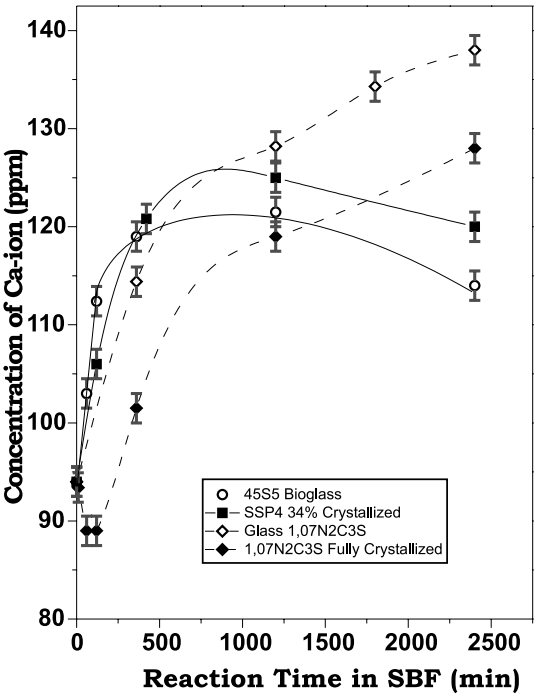

Fig. 8. Calcium ion concentration in reacted SBF-K9 solution for 45S5 Bioglass, SSP4 partially crystallized and 1.07N2C3S glass and glass-ceramic vs. reaction time.

release Ca ions. The more bioactive the material the shorter the time to reach the maximum (Fig. 8).

In compositions containing P_2O_5, phosphorous ions are released very fast (Fig. 7). The P concentration reaches a maximum and then decreases with the development of a Ca–P rich layer, stages IV and V in Fig. 7. Compositions without P_2O_5 show an almost constant concentration of P in the first reaction stages (I to III), which decreases in stages IV and V. The maximum concentration of phosphorous in the solution depends on the SA/V ratio, material composition, and type of solution test. Greenspan [17] has studied the effect of SA/V and concluded that a high SA/V leads to higher concentrations of phosphorous than a low SA/V. Kim et al. [19] have shown that the amount of phosphorous released to the solution and the presence of the maximum are less significant for glasses with higher silica contents.

5. Discussion

In contrast to the work of Li et al. [2], XRD analyses of glass-ceramics SSP4 and SSP6 did not show any crystalline phosphate phase (Fig. 2). This indicates that phosphorus ions stay in solid solution in the 1N2C3S crystal phase, at least for the normal two-step heat treatments used herein. In fact, there is a controversy about the behavior of phosphorous in silicate glass crystallization. Phosphorous ions can substitute for silicon ions in tetrahedral co-ordination in the glasses. However, according to Gonzalez-Oliver [20] and McMillan [21], the double oxygen, P═O, bond is favorable to phosphate phase formation in a silicate network and thus increases the tendency towards crystallization.

To verify the stability of the phosphorous solid solution we performed a test that consisted of submitting samples of fully crystallized (by normal double-stage treatment) SSP4 and SSP6 glass-

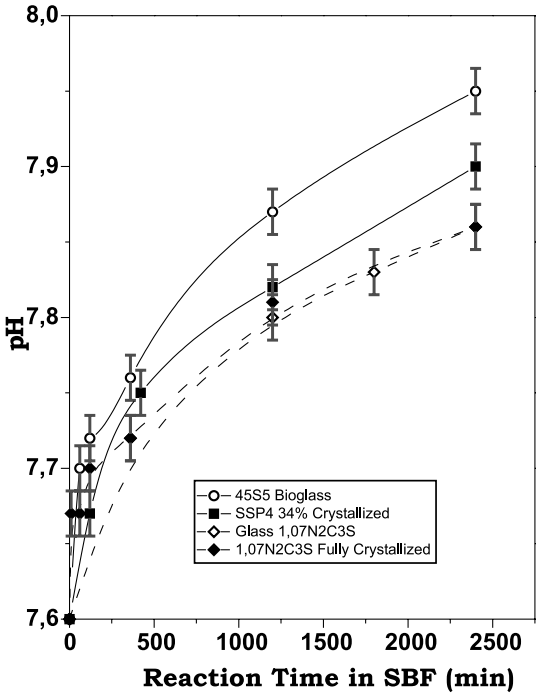

Fig. 9. pH reacted SBF-K9 solution for 45S5 Bioglass, SSP4 partially crystallized and 1.07N2C3S glass and glass-ceramic vs. reaction time.

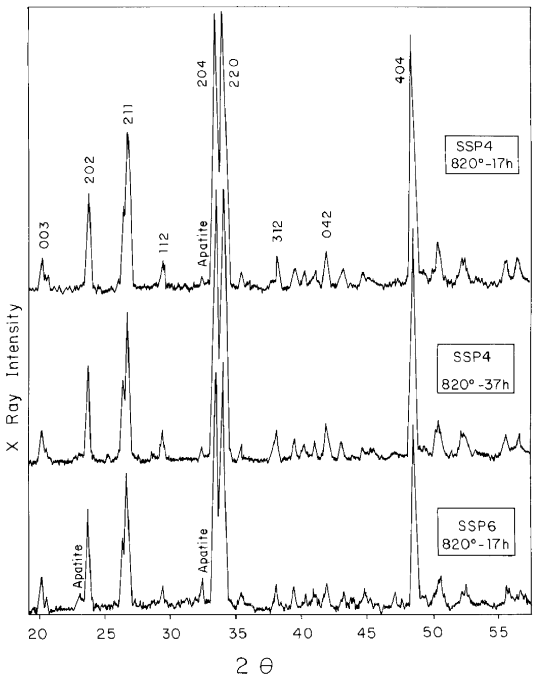

Fig. 10. XRD for SSP4 and SSP6 after third thermal treatment, 17 and 34 h at 820 °C.

ceramics, to very long additional thermal treatments for 17 and 37 h, at a higher temperature, 820 °C. XRD analyses after this third treatment are shown in Fig. 10. The two characteristic phosphate peaks were assigned to an apatite-like phase, similar to that found by Li et al. [2]. Fig. 10 shows that the intensity of these peaks changed slightly from 17 to 37 h of treatment for SSP4, but remained smaller than for SSP6 glass after 17 h at 820 °C.

The FTIR spectra shown in Fig. 11 confirm the presence of an apatite phase in the heat treatment samples only after the third treatment step in a SSP6 glass-ceramic. These results indicate that, in compositions containing up to 6.0% P_2O_5, the phosphorous ions remain in solid solution for ordinary thermal treatments. This procedure is sufficient to produce a fully crystallized glass-ceramic for technical applications. The apatite-like phase precipitated out only under drastic conditions, i.e., after an additional thermal treatment carried out

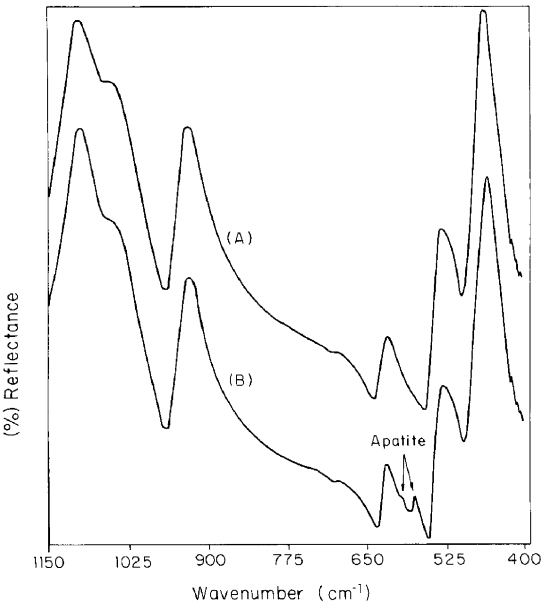

Fig. 11. FTIR spectra for unreacted SSP6 fully crystallized glass-ceramic after heat treatments, (A) double and (B) third, 17 h at 820 °C.

for long time at high temperature. According to Li et al. [2], if the P_2O_5 content is increased to 9%, an apatite-like phase comes out during ordinary crystallization.

The state of the phosphorous ions affects the bioactivity. Glass-ceramics containing an apatite-like phase are several times less reactive than materials containing phosphorous in solid solution, such as 45S5 Bioglass®. The bioactivity level of a fully crystallized glass-ceramic, presented in Fig. 5, shows that phosphorous ions in solid solution, in SSP4 or SSP6, decrease by a factor of 2 to $3x$ the onset time for HCA formation, when compared with SS or 1.07N2C3S. Thus, the presence of phosphorous in solid solution in the glass or glass-ceramic increases the bioactivity level. Fully crystallized SS and 1.07N2C3S glass-ceramics showed similar onset times for HCA formation despite their compositional differences, see Table 2. This behavior was expected because both glass-ceramics are formed by the same single phase 1N2C3S, see Fig. 2. Surface reaction stages are equal for glass and glass-ceramics. They follow the fivestage sequence proposed by Hench and co-authors [3–5] for bioactive glasses. The FTIR spectra, presented in Figs. 3 and 4, show the main surface reactions for HCA layer formation (stages III–V) and they are the same for both glasses and glass-ceramics.

Unreacted surfaces show their natural vibrational modes for the untreated glass (0 h), Fig. 3, and crystal phase 1N2C3S (0 h), Fig. 4. After 7 and 17 h in SBF-K9 (second FTIR spectra in Figs. 3 and 4, respectively) an SiO_2-rich gel layer is formed, stage III, an amorphous $CaO–P_2O_5$-rich layer has started to precipitate (stage IV). The existence of an SiO_2-rich layer is confirmed by the double $Si–O–Si_{(STRETCH)}$ peak at 1250 and 1095 cm^{-1} as well as by the sharpening of the $Si–O–Si_{(BEND)}$ peak at 470 cm^{-1}. Peak development at 780 cm^{-1} is assigned to $Si–O–Si_{(TETRA)}$ vibration between two neighboring SiO_4 tetrahedra. Finally, an Si–O peak at 930 cm^{-1}, present in the unreacted glass spectrum, disappeared with the repolymerization process, stage III. Formation of amorphous $CaO–P_2O_5$-rich film can be observed by a broad peak at 560 cm^{-1}. This peak sharpens as the reaction time increases, followed by the peak at 560 cm^{-1} splitting into two modes, at 602 and 560 cm^{-1}, which are characteristic of an apatite crystalline phase [14]. Splitting of the peaks indicates that the amorphous calcium phosphate film is starting to crystallize, after 9 h on SSP6 glass and 33 h on 1.07N2C3S glass-ceramic. CO_2 is incorporated from the solution, producing a broad peak at 870 cm^{-1}, during crystallization of HCA. At the same time, formation of crystalline HCA on surface produces a $P–O_{(STRETCH)}$ peak at 1050 cm^{-1}.

At the reaction time of HCA crystallization both amorphous and crystalline calcium phosphate layers are very thin and the peaks include a mixture of those from the SiO_2-rich layer (Si–O–Si stretch and bend). However, the $Si–O–Si_{(BEND)}$ peak broadens and the intensity of the $Si–O–Si_{(STRETCH)}$ peak starts decreasing as the HCA phase forms. At this reaction stage there is no difference between the IR spectrum of the SSP6 glass (9 h) and the 1.07N2C3S glass-ceramic (33 h).

As the crystalline calcium phosphate layer grows, the double peaks, $P–O_{(BEND)}$ (560 and 602 cm^{-1}) and $P–O_{(STRETCH)}$ (1050 cm^{-1}), become sharp and dominate the FTIR spectra. Peaks from the SiO_2-rich layer are covered gradually until they disappear, 20 h (glass) and 43 h (glass-ceramic). At this time a third $P–O_{(BEND)}$ peak at 490 cm^{-1} emerges as the characteristic of the well-crystallized HCA layer. After 20 h for glass and 96 h for the 1.07N2C3S glass-ceramic, the FTIR spectra only show peaks assigned to crystalline HCA.

A quantitative analysis of the ions in the solution after in vitro tests is very useful to complement the understanding of surface kinetic reactions in bioactive materials [22]. The highly bioactive material, 45S5 Bioglass®, was used as the standard for comparison with the model glasses and glass-ceramics.

Alkaline and alkaline earth ions are released very rapidly up to 250 min (Fig. 8) to the SBF solution increasing its pH (stage I). Simultaneously, soluble silica forms ($SiOH_4$) in the solution (Fig. 6), decreasing the pH (stage II). The overall pH of the solution (Fig. 9) increases very fast at this time (250 min) dominated by the stage I reaction. After 250 min, the total pH increases

more gradually because the other reaction stages (IV and V) start to occur. In stage IV, part of released calcium is used to form a $CaO–P_2O_5$-rich film, decreasing its release rate (see Fig. 8 compositions without phosphorous). However, compositions containing phosphorous, 45S5 and SSP4, are more bioactive. Thus, a $CaO–P_2O_5$ film crystallized and grew so quickly on these compositions that some calcium ions, used to develop the HCA layer, were withdrawn from the SBF solution after 500 min (Fig. 8). Calcium supply from the bulk material was not sufficient in stages IV and V, for these compositions to maintain growth of the HCA layer and this is the reason for the presence of a maximum on the calcium concentration, Fig. 8, for materials displaying a very high bioactivity level.

Compositions without phosphorous did not show a maximum calcium concentration due to the small thickness of the HCA layer formed. Hence, the amount of calcium released by dissolution was sufficient to maintain the slow rate of growth. There are two experimental facts to support this interpretation; first HCA formation and development depend only on the release of phosphorous from the SBF-K9, less than 30 ppm. Additionally these glasses and glass-ceramics released a very small amount of silica, (Fig. 6) suggesting they are more stable materials and thus produce a thinner SiO_2-rich layer.

An analysis of phosphorous ions in a solution of 45S5 Bioglass® and partially crystallized SSP4 (Fig. 7) shows a very fast dissolution up to 250 min, stage I, increasing the P ion concentration in SBF solution. The subsequent rapid decrease in P concentration indicates the crystallization and growth of the $CaO–P_2O_5$-rich layer. A strong uptake of P occurs when the amorphous calcium phosphate layer crystallizes (after 500 min). Bioglass® 45S5 showed the biggest drop in P ions, indicating a faster HCA layer formation and growth, as expected. Partially crystallized SSP4 showed the same kinetics of dissolution and amorphous $CaO–P_2O_5$-rich film formation, but HCA grew more slowly than on 45S5 Bioglass®.

The 1.07N2C3S glass and glass-ceramic show a similar behavior in the first stages I, II and III (Figs. 7 and 8). The amount of P ion in solution (Fig. 7) was almost constant up to 1000 min because the material cannot dissolve it. Hence, the reaction stages I, II and III occur without the presence of phosphorous. A slight drop is observed between 1000 and 1200 min that indicates the formation of an amorphous $CaO–P_2O_5$-rich film. This agrees with the FTIR spectrum (Fig. 4) after 17 h (1020 min) where a peak appeared at 560 cm^{-1}. The subsequent decrease in P concentration indicates the growth of an amorphous film, which finally crystallizes between 1800 and 2400 min.

The 1.07N2C3S glass and glass-ceramic show only a slight release of silicon ions to the solution, a rate four times slower than SSP4 and 45S5 compositions. This suggests that the Si–O–Si bond in the 1.07N2C3S materials is more difficult to break by the SBF solution than in SSP4 and 45S5 (stage II). One can conclude that 1.07N2C3S forms a thinner SiO_2-rich layer, and therefore is less bioactive. This conclusion is supported by the results of Fig. 5, where the onset time of HCA formation is the longest for 1.07N2C3S glass-ceramic.

Comparing the ions released from partially crystallized SSP4 and 45S5 Bioglass® we conclude that they had a very similar behavior in terms of the kinetics of HCA layer formation. A slight difference in solubility and rate of HCA formation was observed in favor of 45S5. This is an important fact because *the glass-ceramic developed* is a *unique crystalline material* having comparable bioactivity behavior to 45S5 Bioglass® *but substantially superior mechanical properties* [1,16,23]. Therefore using in vitro data collected in our research, we conclude that SSP4 and SSP6 bioglass and glass-ceramics developed can be classified as class A bioactive material, according to Hench's [15] criteria.

Glass and glass-ceramic 1.07N2C3S showed similar reactions of HCA layer formation, Figs. 5–9. *This indicates a surprising fact that crystallization did not affect significantly the kinetic reactions in this family of glasses.* Even in the absence of phosphorous they are much more bioactive than other commercial bioactive glass-ceramics.

6. Conclusions

Controlled crystallization produced single-phase glass-ceramics for all compositions studied. The crystal phase was identified as $1Na_2O \cdot 2CaO \cdot 3SiO_2$. For compositions containing phosphorous, SSP4 and SSP6, an apatite-like phase was detected after a third treatment in drastic conditions, i.e., long times at a high temperature.

From ion solution measurements after in vitro tests, it was possible to identify the five reaction stages leading to HCA formation that correlated with changes in FTIR spectra.

All compositions developed a HCA layer when submitted to in vitro tests in SBF-K9 solution. The FTIR and ICP analysis demonstrated that both glass and glass-ceramics formed a HCA layer according to the mechanism proposed by Hench et al. [3–5]. Hence the glasses and glass-ceramics are bioactive materials.

The effect of volume fraction of crystal phase on the kinetics of HCA formation was small. Even phosphorous-free compositions were able to form a HCA layer by incorporating P ions from the simulated physiological fluid. In vitro tests demonstrated that fully crystallized ceramics, SS and 1.07N2C3S, are less bioactive than the parent glasses, however, they are much more bioactive than commercial bioactive ceramics and glass-ceramics. This fact indicates that the crystal phase $1Na_2O \cdot 2CaO \cdot 3SiO_2$ has a high bioactive index.

Crystallization increases the onset time for HCA formation up to three to four times for compositions with phosphorous, but they still remained bioactive. The bioactivity behaviors of SSP4 and SSP6 glass and glass-ceramics were quite similar, despite the difference in phosphorous concentration.

Acknowledgements

The authors gratefully acknowledge the financial support of the Conselho Nacional de Desenvolvimento Científico Tecnológico, CNPq/CYTED, FAPESP, PRONEX (Brazil) and the Air Force Office of Scientific Research (USA), grant #F49620-92-J-0351.

References

[1] O. Peitl, G. La Torre, L.L. Hench, J. Bio. Mater. Res. 30 (1996) 509.
[2] P. Li, F. Zhang, T. Kokubo, J. Mater. Sci. Mater. Med. 3 (1992) 452.
[3] L.L. Hench, in: Joy E. Hulbert, Samuel F. Hulbert (Eds.), Bioceramics, USA, vol. 3, 1991, p. 43.
[4] L.L. Hench, Ö.H. Andersson, G. La Torre, in: W. Bonfield, G.W. Hastings, K.E. Turner (Eds.), Bioceramics, UK, vol. 4, 1991, p. 155.
[5] L.L. Hench, G. La Torre, in: T. Yamamuro, T. Kokubo, T. Nakamura (Eds.), Bioceramics, Japan, vol. 5, 1992, p. 67.
[6] O.K. Nakamura, T. Yamamuro, Y. Ebisawa, T. Kokubo, Y. Kotoura, M. Oka, J. Mater. Sci. Mater. Med. 3 (1992) 95.
[7] K. Hyakuna, T. Yamamuro, Y. Kotoura, M. Oka, T. Kokubo, in: T. Yamamuro, L.L. Hench, J. Wilson (Eds.), Handbook of Bioactive Ceramics, vol. 1, CRC, Boca Raton, FL, 1990, p. 125.
[8] M.R. Filqueiras, G. La Torre, L.L. Hench, J. Biomed. Mater. Res. 27 (1993) 1485.
[9] W. Höland, W. Vogel, K. Naumann, J. Gummel, J. Biomed. Mater. Res. 19 (1985) 303.
[10] M.U. Gross, V. Strunz, J. Biomed. Mater. Res. 15 (1981) 291.
[11] T. Kokubo, H. Kushitani, S. Sakka, J. Biomed. Mater. Res. (1990) 721.
[12] L.L. Hench, in: P. Ducheyne, J.E. Lemons (Eds.), Annuals of New York Academy of Science, vol. 523, 1988, p. 54.
[13] A.E. Clark, L.L. Hench, J. Non-Cryst. Solids 113 (1989) 195.
[14] G. La Torre, L.L. Hench, in: J.H. Adair, J.A. Casey (Eds.), Characterization Methods for the Solid–Solution Interface in Ceramic System, American Ceramic Society, Westerville, OH, 1993.
[15] L.L. Hench, Bioceramics: theory and clinical applications, bioceramics, in: O.H. Andersson, A. Yli-Urpo (Eds.), Proceedings of the 7th International Symposium on Ceramics in Medicine, Turku, vol. 7, July 1994, p. 3.
[16] L.L. Hench, O. Peitl, G. La Torre, E.D. Zanotto, Bioactive Ceramics and Method of Preparing., USPTO: US5981412, May, 1, 1997 and European Patent Office: 97925614.6-2111, Dec., 8, 1997. States AT, BE, CH, DE, DK, ES, FI, FR, GB, GR, IE, IT, LI, LU, MC, NL, PT and SE.
[17] D.C. Greenspan, J.P. Zhong, G. La Torre, in: Ö.H. Anderson, Yli-Urpo (Eds.), Bioceramics, Turku, Finland, vol. 7, 1994, p. 55.
[18] G.K. Moir, F.P. Glasser, Phys. Chem. Glasses 15 (1) (1974) 6.

[19] C.K. Kim, A.E. Clark, L.L. Hench, J. Biomed. Mater. Res. 26 (1992) 1147.
[20] C.J.R. Gonzalez-Oliver, PhD thesis, University of Sheffield, UK, 1979, p. 175.
[21] P.W. McMillan, in: J.P. Roberts, P. Popper (Eds.), Glass-ceramics, 2nd Ed., Academic Press, New York, 1979, p. 76.
[22] L.L. Hench, J. West, Biological applications of bioactive glasses, Life Chemistry Reports, vol. 13, 1996, p.187.
[23] O. Peitl, PhD thesis, UFSCar, Brazil, 1995, p. 370.